JOURNAL OF OPTOELECTRONICS AND ADVANCED MATERIALS, Vol. 10, No. 10, October 2008, p. 2663 - 2666

Observation of nanorods in tungsten-oxide powders annealed at 200°C

K. GEORGE VARGHESE[a,b*], V K VAIDYAN[a,c]
[a]*Department of Physics, University of Kerala, Trivandrum-695 581, INDIA*
[b]*Department of Physics, St.Gregorios College, Kottarakkara- 691 531, Kerala, INDIA*
[c]*Department of Physics, Fatima Mata national College, Kollam-691 001, Kerala, INDIA*

Tungsten trioxide (WO_3) nanorods are observed for the first time at a lower temperature, when nanosized powder sample of WO_32H_2O was annealed at 200°C for 30 minutes. More than 50% of the nanoparticles in the powder sample were converted into nanorods. The nanorods and nanoparticles are characterized by X-ray diffraction (XRD) and high resolution transmission electron microscopy (HRTEM) as crystalline with primitive cubic tungsten trioxide (c-WO_3).

(Received March 18, 2008; accepted August 14, 2008)

Keywords: WO_3 nanorods, Nanoparticles, Tungsten trioxide

1. Introduction

Transition metal oxides represent a large family of materials possessing various interesting properties, such as superconductivity, colossal magneto-resistance and piezoelectricity. Tungsten trioxide (WO_3) has received much attention because of its potential for many technological applications, such as electrochromic devices, gas sensors and varistors [1-3]. Recently, current-voltage measurement systems using multiple probes have been developed for nanoscale electrical measurements. There has been a few reports on using nanorods of WO_3 as STM probes [4]. Nanorods of WO_3 were prepared by different methods [5-7]. Here, a study on the formation of WO_3 nanorods at 200°C with tungsten trioxide dihidrate (WO_32H_2O) as the starting material is reported. Studies on the formation of nanorods in samples annealed at other temperatures are progressing.

2. Experimental

Tungsten trioxide dihydrate (WO_32H_2O) precursor for the preparation of tungsten trioxide (WO_3) nanorod was synthesized through a controlled chemical precipitation route employing aqueous solution of sodium tungstate and hydrochloric acid. The as prepared precursor sample was dried at 40°C and was finely grounded and annealed at 200°C for 30 minutes. XRD pattern of the sample was recorded for 2θ range from 3 to 80° using Philips X-ray diffractometer using CuKα radiation. High Resolution Transmission Electron Microscopic analysis of the sample was done using the JEOL microscope (Model JEM 3010 300kV) operating at an accelerating voltage of 200 kV.

3. Results and discussion

The crystalline phase of WO_3 was identified from the XRD pattern by comparing with the ICDD standard and the average crystallite size of the phase was estimated from the most intense peak in the diffraction pattern using Scherrer equation [8],

$$D = \frac{k\lambda}{\beta \mathrm{Cos}\theta}, \quad (1)$$

where k is a constant (for spherical particles k = 0.9) and β is the full width at half maximum of the diffraction peak and θ is the diffraction angle and λ = 0.15418 nm for Cu K_α . The XRD pattern of the sample shown in Figure 1 contains peaks corresponding to the cubic phase of WO_3 (ICDD file no: 41-905). The grain size of the sample calculated by using Equation (1) is 11 nm.

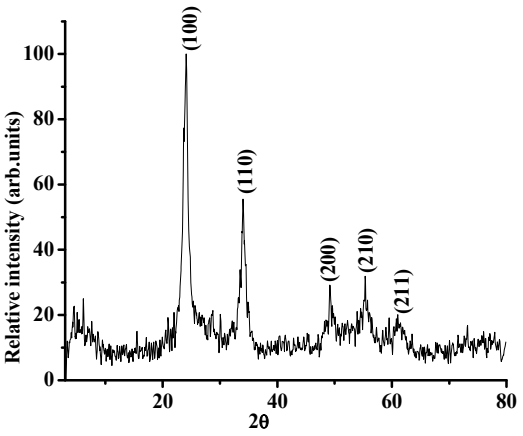

Fig. 1. XRD pattern of the sample.

From the HRTEM images of Fig. 2, it can be seen that the sample consists of grains associated as agglomerates and as separate particles of size ranging from 10 to 30 nm. Further, more than 50% of the particles are converted into nanorods. The direction of growth of each nanorod is observed to be parallel to each other. The SAED pattern of a grain shown as inset of Fig. 3 and of the nanorod given as inset of Fig. 4 show crystalline nature for the grains and the nanorods. The SAED pattern of nanorod is rich in spots than the SAED pattern of the grain which is more of a ring-like structure. The difference in the appearance of the SAED pattern shows that nanorods are not formed out of smaller-sized particles in the distribution.

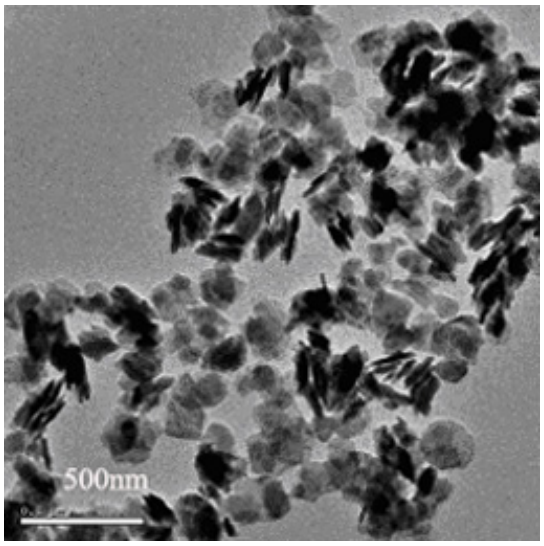

a

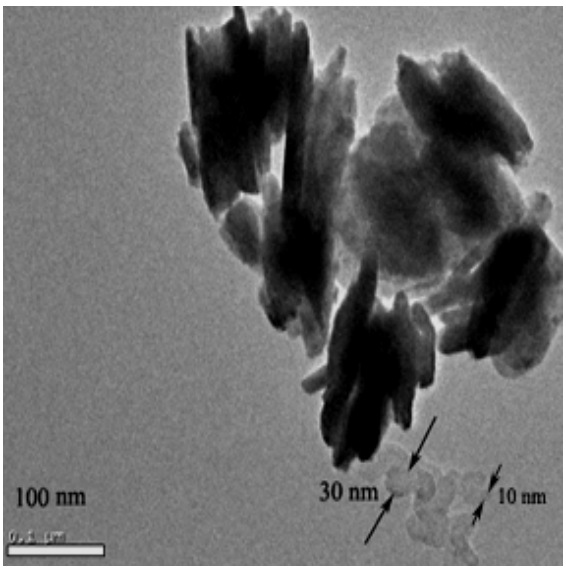

b

Fig. 2. HRTEM images of WO_3 nano particles and nanorods showing (a) grains associated as agglomerates and nanorods, and (b) nanorods of length up to 200 nm and diameter ~18 nm and nanoparticles of spherical shape with grain size10 to 30 nm.

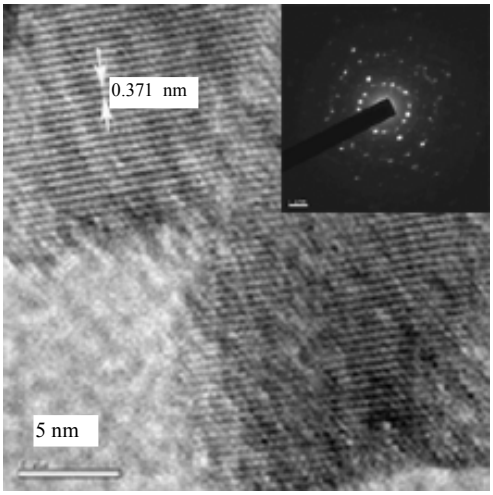

Fig. 3. Atomic scale image of powder particles in the sample with the (100) plane and the inset shows SAED pattern of a grain.

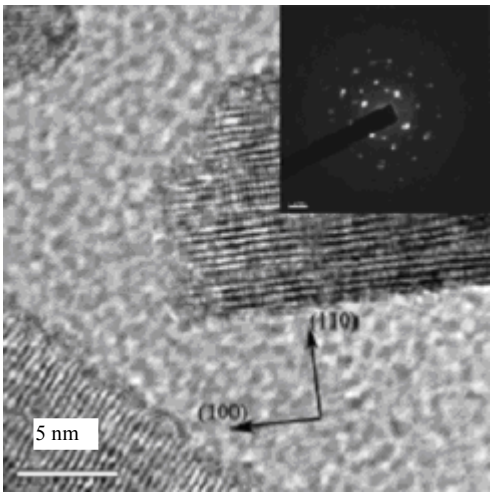

Fig. 4. HRTEM lattice fringe image of a nanorod in the sample with the inset showing SAED pattern of a nanorod.

The SAED pattern of grain shown as inset of figure 3 and that of the nanorod given as inset of figure 4 show crystalline nature for the grains and the nanorods. The SAED pattern of nanorod is rich in spots than the SAED pattern of the grain which is more of a ring-like structure. The difference in the appearance of the SAED pattern shows that nanorods are formed out of larger-sized particles in the distribution.

From the SAED pattern, it is evident that the grains and nanorods in the sample consist of nanoparticles of WO_3 with primitive cubic crystal structure. This observation is confirmed from the XRD pattern of this sample. In the lattice fringe image given in Figure 3, lattice fringes are observed at intervals of 3.71 A^o for most of the grains. This lattice spacing coincides with $d_{(100)}$ spacing of cubic WO_3.

In Fig. 4, the amorphous region surrounding the nanorod, bonding the rod with the surrounding grains can be seen. From the lattice fringes observed on the rod, the major direction of growth of nanorod is found to be perpendicular to d_{110} plane and parallel to d_{100} plane of cubic WO_3. XRD pattern of the sample shows that (100) and (110) peaks are stronger than the rest suggesting the major direction of growth as (100) [9]. From the HRTEM image of the single nanorod shown in figure 5(a), the following observations can be made from the geometry of the nanorod. The corners of the rod are faceted and the cross section is uniform except at the top end. The non uniform cross section of the top end suggests the existence of a strong driving force for growth (growth along the direction of the arrow given as 'c') even though there is a pressure from the nearest surface, which is indicated by the deformation indicated by the arrow 'a'. The pressure inside the nanorod exhausts through no-thrust regions. This can be observed as a slight bulging region and is indicated by the arrow 'b'.

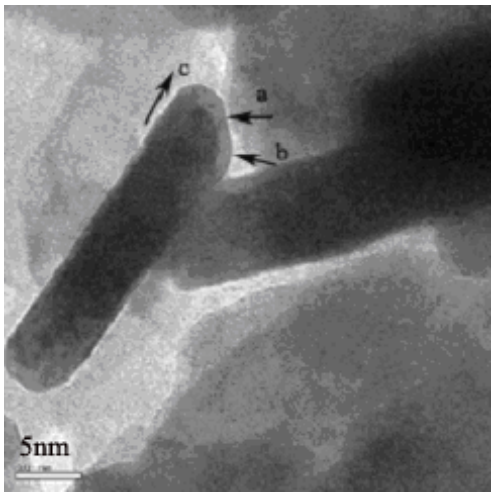

a

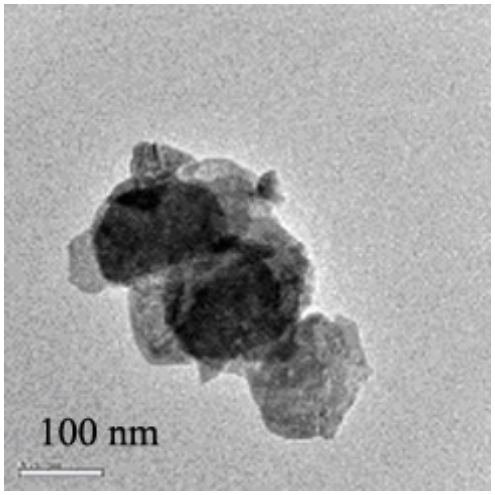

b

Fig. 5. HRTEM image of (a) a single nanorod and (b) agglomorates arranged one dimensionally.

To account for the mechanism of one dimensional growth, the Vapour-Liquid-Solid (VLS) model was proposed by Wagner and Ellis in 1964 [10], which is the fundamental mechanism by which materials grow one dimensionally as wires, whiskers or rods. In all the reported HRTEM images of WO_3, grains are observed to be associated as agglomerates and it is difficult to locate individual particles. The surface energy of the nanoparticles being high, there is a natural tendency for nanoparticles to reduce their energy by coalation of individual spherical grains. In Figure 5(b), we can see one dimensional agglomeration of similar-sized clusters, that may be the first stage in the development of a nanorod. Once the initial structure for a nanorod is formed by the agglomoration of similar-sized clusters one dimensionally, excess pressure generated inside the structure due to coalescing initiates growth of a nanorod, similar to rise of liquid in a capillary tube. Water present in the starting material imparts enough mobility to the spherical nanoparticles in the sample. The pressure from out side, as seen in Figure 5(a), restricts the growth to be one dimensional. The length of the nanorod is decided by the dimension along the growth direction, where the force due to excess pressure inside the rod is balanced by the external deforming force towards the structure. We further observe that nanorods are not formed at every location, but only where certain cluster arrangements are present. This can be attributed to certain critical size requirement of the clusters for the formation of nanorods. The distribution of particle sizes is clear from Figure 2(b). The existence of size distribution and selective formation of nanorods at certain locations and the bigger-sized particles in nanorods support the idea that a critical size is necessary for the formation of nanorods. The possibility of vapor or liquid phase of WO_3 at the annealing temperatures is rare since the melting point of WO_3 is 1473°C.

In order to verify whether the growth of nanorods is through melting of the sample, the precursor sample was sintered at 1000°C for two hours, when an increase in grain size was observed, but no melting of the sample has occurred. Thus, samples are in solid phase at the nanorod development stage, with some water around it, emanating from the starting materials as starting material used for the preparation of the sample was $WO_3 2H_2O$. In addition, the sample showed presence of structural water according to its FTIR and FT Raman results. No catalyst was used during the preparation of the sample. Thus, the influence of water present in the starting material alone is to be considered in the growth of nanorods.

The VLS growth mechanism has been widely used to guide the growth of various kinds of nanostrutures such as carbon nanotubes [11-13], nanowires of semiconductors [14] and oxides [15]. As reported by Kunquan Hong et.al. [9], presence of water promotes the development of nanostructures and in the presence of potassium iodide (KI) as catalyst they succeeded in the large scale production of nanorods. At high temperatures, nanstructures were reported [16] in the presence of water even without a catalyst. It can be concluded that in the

absence of a catalyst, nanorods are formed at low temperatures, which can be considered as the unique property of nanomaterials. Association of grains into agglomerates, assisted by water molecules paves the way for creation of nanorods. When agglomerates of WO_3 of critical size arrange one dimensionally, nucleation sites for the creation of nanorods are generated. Once the nucleation site is formed, smaller grains of critical size, instead of gas phase or liquid phase component, attach itself to the site and as a result of the forward force and lateral pressure, growth of nanorods proceed. This situation is satisfactorily completed for a number of agglomerates in the sample.

4. Conclusion

Tungsten trioxide (WO_3) nanorods are formed when grains of critical size agglomerates, assisted by water molecules one dimensionally, and act as nucleation sites for nanorod formation. Excess liquid or gas phase is not present, smaller grains gets attached to the nucleation sites to complete the structure of a rod. Crystal structure of nanorods and nanoparticles in the sample is the same. Further, adjacent nanorods grow in parallel directions.

Acknowledgements

One of the authors (KGV) is thankful to University Grants Commission, New Delhi, for the award of a fellowship under the Faculty Improvement Programme

References

[1] X. S. Yang, M. Chen, Y Wang, Acta Phys. Sin. **52,** 1545 (2003)
[2] C. G. Granqvist, Solar Energy Mater. Solar Cells **60,** 201 (2000)
[3] Z. L. Liu, L. F. Yang, Y, Wang, Chin. Phys. **13,** 384 (2004)
[4] O. Kubo, Y. Shingaya, M. Nakaya, M. Aono, T. Nakayamab, Appl.Phys.Lett. **88,** 254101 (2006)
[5] B. C. Satishkumar, A. Govindaraj, Manashi Nath, C. N. R. Rao, J. Mater. Chem. **10,** 2115 (2000)
[6] B. Li, Y. Bando, D. Golberg, K. Kurashima, Chem. Phys. Lett. **367,** 214 (2003)
[7] S. V. Pol, V. G. Pol, V. G. Kessler, G. A. Seisenbaeva, L. A. Solovyov, A. Gedanken, Inorg. Chem. **44,** 9938 (2005)
[8] P. Scherror, Gottinger Nachrichten **2** 98 (1918)
[9] Kunquan Hong,Wingching Yiu, HuashengWu, Ju Gao, Maohai Xie, Nanotechnology **16** 1608 (2005)
[10] R. S. Wagner, W. C. Ellis, Appl.Phys.Lett. **4,** 89 (1964)
[11] Z. W. Pan, S. S. Xie, B. H. Chang, C. Y. Wang, L. Lu, W. Liu, W. Y. Zhou, W. Z. Li W, L. X. Quian, Nature **394** 631 (1998).
[12] S. S. Fan, M. G. Chapline, N. R. Franklin, T. W. Tombler, A. M. Casell, H. J. Dai, Science **283,** 512 (1999)
[13] B. Chen, P. Wu, Carbon **43** 3172 (2005)
[14] X. F. Duan, C. M. Lieber, 2000 Adv.Mater. **12** 298 (2000).
[15] M. Huang, S. Mao, H. Feick, H. Yan, Y. Wu, H. Kind, E. Weber, R. Russo, P. Yang, Science **292,** 1897 (2001)
[16] Y. Z. Jin Y, et al J. Phys. Chem. B **108,** 15572 (2004)

*Corresponding author: gvkilivayal@yahoo.co.in